The humanin analogue (HNG) prevents temozolomide-induced male germ cell apoptosis and other adverse effects in severe combined immuno-deficiency (SCID) mice bearing human medulloblastoma

Yue Jia[a], Yanhe Lue[a], Ronald S. Swerdloff[a], Joseph L. Lasky[b], Eduard H. Panosyan[b], Jenny Dai-Ju[a], Christina Wang[a,*]

[a] Division of Endocrinology, Department of Medicine, Los Angeles Biomedical Research Institute and Harbor-UCLA Medical Center, Torrance, CA, United States of America
[b] Division of Pediatric Hematology and Oncology, Department of Pediatrics, Los Angeles Biomedical Research Institute and Harbor-UCLA Medical Center, Torrance, CA, United States of America

ABSTRACT

Subfertility is a major concern of long-term cancer survivors at the reproductive age. We have previously demonstrated that a potent humanin analogue, HNG, protected chemotherapy-induced apoptosis in germ cells but not cancer cells in a metastatic melanoma allograft model. In this study, we utilized severe combined immuno-deficiency (SCID) mice bearing human medulloblastoma to study the effect of HNG in Temozolomide (TMZ) induced male germ cell apoptosis and white blood cell (WBC) suppression. Human medulloblastoma DAOY cells were injected subcutaneously into the right flank of male SCID mice. Three weeks later, groups of tumor-bearing mice received one of the following treatments: vehicle, HNG, TMZ, or TMZ + HNG. 24 h after last injection, the tumors weights, complete blood counts, liver and spleen weights, male germ cell apoptosis was assessed. HNG did not affect TMZ's significant anti-tumor action. HNG significantly prevented TMZ-induced germ cell apoptosis and attenuated the suppressed total WBC and granulocyte counts in SCID mice with or without TMZ treatment. HNG also attenuated TMZ-induced body weight loss and decrease of spleen and liver weights. In conclusion, HNG ameliorated TMZ-induced germ cell apoptosis; WBC and granulocytes loss; and decreased body/organ weights without compromising the TMZ's anti-cancer action on medulloblastoma xenografts in SCID mice.

1. Introduction

Humanin (HN), a mitochondrial derived 24-amino acid peptide, prevents cell damage from stress/injury in different tissue/cells, including neuronal tissue (Hashimoto et al., 2001; Matsuoka, 2009; Xu et al., 2006), heart and blood vessel (Bachar et al., 2010; Muzumdar et al., 2010), bone (Eriksson et al., 2014), blood-derived cells (Wang et al., 2005; Ying et al., 2004) and white blood cells (Lue et al., 2015), pancreas (Muzumdar et al., 2009; Hoang et al., 2010), and male germ cells (Lue et al., 2015; Lue et al., 2010; Jia et al., 2013; Jia et al., 2015). Our prior published work showed that male germ cell apoptosis can be induced in rodents (Sinha Hikim et al., 1995; Lue et al., 1999; Cai et al., 1997), monkeys (Lue et al., 2006; Jia et al., 2007), and men (Wang

et al., 2007) by a variety of apoptotic stimuli including testicular hyperthermia, administration of insulin-like growth factor binding protein 3 (IGFBP-3), hormone deprivation, and chemotherapeutic drugs (Lue et al., 2015; Jia et al., 2013; Jia et al., 2015; Sinha Hikim et al., 1995; Lue et al., 1999; Cai et al., 1997; Lue et al., 2006; Jia et al., 2007; Wang et al., 2007). Administration of HN or potent analogue HNG (where the serine in position 14 of humanin is substituted by glycine) prevents heat, IGFBP-3, GnRH-Antagonist, or cyclophosphamide induced male germ cell apoptosis in rodents (Lue et al., 2015; Lue et al., 2010; Jia et al., 2013; Jia et al., 2015).

Modern chemotherapies have changed the prognosis of cancer patients with dramatically increased survival and life expectancy. Infertility or sub-fertility is one of major concern of pediatric cancer

survivors (Marcon et al., 2008; Meistrich, 2009; Lee and Shin, 2013). Accordingly, we explored the role of HNG in preventing male germ cell apoptosis and other side effects induced by chemotherapeutic drug, Temozolomide (TMZ), an alkylating agent commonly used in pediatric brain cancers in an immunocompromized mouse models (Villano et al., 2009; Friedman et al., 2000). In this study, we investigated whether the HNG alters the TMZ-induced tumor suppression and its possible protective effects in male germ cells, white blood cells, and other organs against TMZ-induced toxicity.

2. Materials and methods

2.1. Materials

TMZ was obtained from Sigma (St. Louis, MO) and dissolved in dimethyl sulfoxide (DMSO). HNG peptide was synthesized by CPC Scientific (Sunnyvale, CA) and dissolved in 0.9% saline. In this study, the effect of HNG was studied using TMZ treated mouse model bearing human medulloblastoma.

2.2. DAOY cell line culture

We used DAOY cell which is a pediatric medulloblastoma cell line with moderate TMZ sensitivity (von Bueren et al., 2012) in a well-established xenotransplant tumor model in severe combined immunodeficient (SCID) mouse (Jacobsen et al., 1985). DAOY [ATCC® HTB-186™] cell line was purchased from American Type Culture Collection (Manassas, VA) and verified according to the ATCC procedures.

2.3. Animals experiments

Male SCID mice 7-week-old at the time of tumor cells implant (obtained from The Jackson Laboratory, Bar Harbor, Maine) were housed in a standard animal facility under controlled temperature (22 °C) with photoperiod of twelve hours of light and twelve hours of darkness with free access to food and water. Animal handling and experimentation were in accordance with the recommendation of American Veterinary Medical Association and were approved by the animal care and use review committee at the Los Angeles Biomedical Research Institute at Harbor-University of California, Los Angeles (Harbor-UCLA) Medical Center.

Tumor cells (1×10^8) were injected under the skin in the right flank in mice ($n = 20$ in total). Three weeks after implantation, animals ($n = 5$ each group) were pre-treated with intraperitoneal (IP) injections of saline or HNG for 3 days and then treated with HNG and/or TMZ for another 5 days as follows: 1) Controls received daily (IP) injection of normal saline for 3 days pretreatment plus 5 days treatment with saline and DMSO; 2) HNG group received daily IP injection 5 mg/Kg BW for 3 days before TMZ and 5 days with TMZ; 3) TMZ group received daily IP injection TMZ 50 mg/Kg BW for 5 days treatment), and 4) TMZ and HNG received both treatment at the same doses and for the same schedule as above.

Tumors were measured with digital caliper thrice a week. Animals were euthanized if tumors reached 1.5 cm in length. An ellipsoid volume formula was used to calculate tumor volumes (1/2 × length × width^2) (Reynolds et al., 2005). Mice were weighed 2 to 3 times per week throughout the whole experiment. One mouse in non-treated (control) group was found dead due to accidental trauma 5 days before the end of the experiment.

2.4. Blood collection and tissue preparation

As described previously (Lue et al., 2015), mice were injected with heparin (1300 IU/kg BW, IP) 15 min before sacrifice by a lethal injection of sodium pentobarbital (200 mg/kg BW, IP). Blood samples were collected from the right ventricle of each mouse immediately after death and used for complete blood count (CBC) using an automated cell counter (VetScanHM2, ABAXIS, Union City, CA). In two mice, one in non-treated (control) group and one in TMZ group, we were unable to perform CBC counting due to hemolysis of the blood cells during blood collection.

One testis from each mouse was removed, weighed, and snap-frozen into liquid nitrogen, the other was fixed in Bouins' fixative (Newcomer Supply, Middleton, WI), paraffin embedded for TUNEL assay. Subcutaneous tumor in the right flank, liver and spleen from each mouse were weighed and then fixed with Zinc-Formalin (Fisher Diagnostics, Middletown, VA) and part of the liver and spleen were snap-frozen for immunoblots.

2.5. Assessment of germ cell apoptosis in testis

Assessing of apoptotic germ cell was performed in testicular sections by the terminal deoxynucleotidyl transferase (TdT)-mediated deoxy-UTP nick end labeling (TUNEL) technique (Sinha Hikim et al., 1997) using an ApopTag-peroxidase kit (Chemicon International, Inc., Temecula, CA). Enumeration of the apoptotic germ cell population and Sertoli cell nuclei with distinct nucleoli was quantified at stages I-IV (early stages), stages VII-VIII (middle stages), and stages XI-XII (late stages) of the seminiferous epithelial cycle by using an Olympus BH-2 microscope (New Hyde Park, NY). Stages were identified according to the criteria proposed by Russell et al. for paraffin sections (Russell, 1977). The rate of germ cell apoptosis was expressed as the number of apoptotic germ cells per Sertoli cell (apoptotic index, AI) (Sinha Hikim et al., 1997).

2.6. Subcellular fractionation and Western blotting analysis

Cytosolic and mitochondrial fractions of testis were prepared as described previously (Jia et al., 2007). Briefly, frozen testis tissue was homogenized in 0.3 ml buffer A (0.25 M sucrose, 50 mM Hepes, 10 mM NaCl, 10 mM EDTA, 2 mM dithiothreitol) supplemented with protease inhibitors (Complete Protease Inhibitors, Roche, Risch-Rotkreuz, Switzerland). The crude homogenates were centrifuged at 1000g for 10 min at 4 °C, and the resultant supernatant centrifuged at 10,000g for 15 min at 4 °C to sediment the low-speed fraction containing mainly mitochondria. The mitochondria were washed twice in buffer A and pelleted. The cytosolic and high-speed fractions were isolated following centrifugation of the 10,000g supernatant fraction at 100,000 g for 60 min at 4 °C. The resulting supernatant was the cytosolic fraction. The RIPA buffer (Santa Cruz Biotechnology, Santa Cruz, CA) was added in fractions. Total lysates of liver and spleen were prepared with similar methods without centrifuge. Briefly, liver and spleen were homogenized in buffer A (see above) supplemented with protease inhibitors and the RIPA buffer was added after homogenization.

Western blotting was performed as described previously (Jia et al., 2009). In brief, proteins were denatured and separated by sodium dodecyl sulfate-polyacrylamide gel electrophoresis (SDS-PAGE) system (Invitrogen, Carlsbad, CA). After transferring, the Immuno-blot PVDF Membrane (Bio-Rad, Hercules, CA) was blocked for 1 h and then probed using anti-STAT3, pSer727 STAT3, cleaved PARP (Poly(ADP-ribose) Polymerase), COX IV (Cell signaling Technology, Inc., Beverly, MA), BAX, Cytochrome C, PARP, or GAPDH (Santa Cruz Biotechnology, Dallas, TX) overnight at 4C with constant shaking. After washing, membrane was then incubated with an anti-mouse (for STAT3 or GAPDH antibody, Santa Cruz Biotechnology, Santa Cruz, CA) or anti-rabbit (for pSer727 STAT3, cleaved PARP, PARP, BAX, Cytochrome C, or COX IV antibody, Amersham Biosciences, Piscataway, NJ) IgG-HRP secondary antibody. All antibodies were diluted in blocking buffer. For immunodetection, membrane was incubated with enhanced chemiluminescence solutions per the manufacturer's specifications (Amersham Biosciences, Piscataway, NJ), and exposed to Hyperfilm ECL (Denville Scientific Inc., Metuchen, NJ).

2.7. Measurements of P38 MAPK activation

We have previously shown that activation p38 PMAK is an upstream pathway leading to male germ cell apoptosis (Jia et al., 2009). Activity of p38 MAPK was measured by using assay kit (Cell Signaling Technology Inc., Beverly, MA) as described previously (Jia et al., 2015). In brief, a monoclonal phospho-specific antibody to p38 MAPK (Thr180/Tyr182 phosphorylated) was used to selectively immunoprecipitate active p38 MAPK from whole testis lysates. Then the resulting immunoprecipitate was incubated with activating transcription factor 2 (ATF2) fusion proteins and ATP in kinase reaction buffer, which allows immunoprecipitated active p38 MAPK to phosphorylate ATF2. Phosphorylated ATF2 was assessed by Western blotting with phospho-ATF2 (Thr71) antibody (provided in the p38 MAPK activity assay kit, Cell Signaling Technology Inc., Beverly, MA). ATF2 was used as loading control and normalizer.

2.8. Statistical analysis

Statistical analyses were performed using the SigmaStat 12.0 Program (Systat Software Inc., San Jose, CA). Data are presented as mean ± SEM, and analyzed by one-way ANOVA, and post-hoc tests by Tukey-Kramer correction for multiple comparisons. Differences were considered significant if $P < .05$.

3. Results

3.1. HNG reversed TMZ-induced decrease in body and organs weights

Mice treated with TMZ lost more body weight compared with mice in control or HNG groups fed the same diet (Fig. 1A, overall group comparison $P < .05$). HNG prevented body weight loss induced by TMZ. The change in body weight of HNG + TMZ treated mice was not significantly different from control or HNG treated groups (Fig. 1A, $P > .05$).

HNG treatment increased spleen weight while TMZ significantly decreased spleen weight (Fig. 1B, compared with control group $P < .05$ for both groups). HNG treatment prevented the TMZ-induced decrease in spleen weights restoring to control values (Fig. 1B).

HNG treatment did not change but TMZ significantly decreased liver weight of SCID mice (Fig. 1C, compared with control group $P < .05$). HNG co-administration attenuated the liver weight reduction induced by TMZ (Fig. 1C, overall group comparison $P < .05$).

3.2. TMZ-induces changes in cleaved PARP and phosphorylation STAT3 were reversed by HNG in mouse liver and spleen

We have previously shown that phosphorylation of Ser727 or Tyr705 to activates STAT3 is one of the main signal pathway of HNG action (13–14). We also used cleaved PARP as a marker for apoptosis in liver and spleen of SCID mice. In liver tissue, immuno-blot showed that HNG did not change cleaved PARP but TMZ increased levels of cleaved PARP (Fig.2A, $p < .05$ compared with control group). Co-treatment with HNG prevented TMZ-induced increase in cleaved PARP levels (Fig. 2A, $p < .05$ compared with TMZ alone group). TMZ treatment suppressed Ser727-phosphorylated STAT3 in liver (Fig.2B, $p < .05$ compared with control group). HNG administration restored TMZ-suppressed Ser 727-phosphorylation of STAT3 (Fig. 2B, $p < .05$ compared with TMZ alone group).

In spleen tissue, HNG suppressed cleaved PARP levels compared with control group (Fig.2C, $p < .05$). TMZ group did not increased cleaved PARP compared with control (Fig.2C, $p > .05$). HNG administration also attenuated TMZ-increased cleaved PARP levels (Fig. 2C, $p < .05$ compared with TMZ alone group). HNG increased STAT3 phosphorylation in spleen compared with control group (Fig.2D, $p < .05$). HNG administration restored TMZ-suppressed Ser 727-
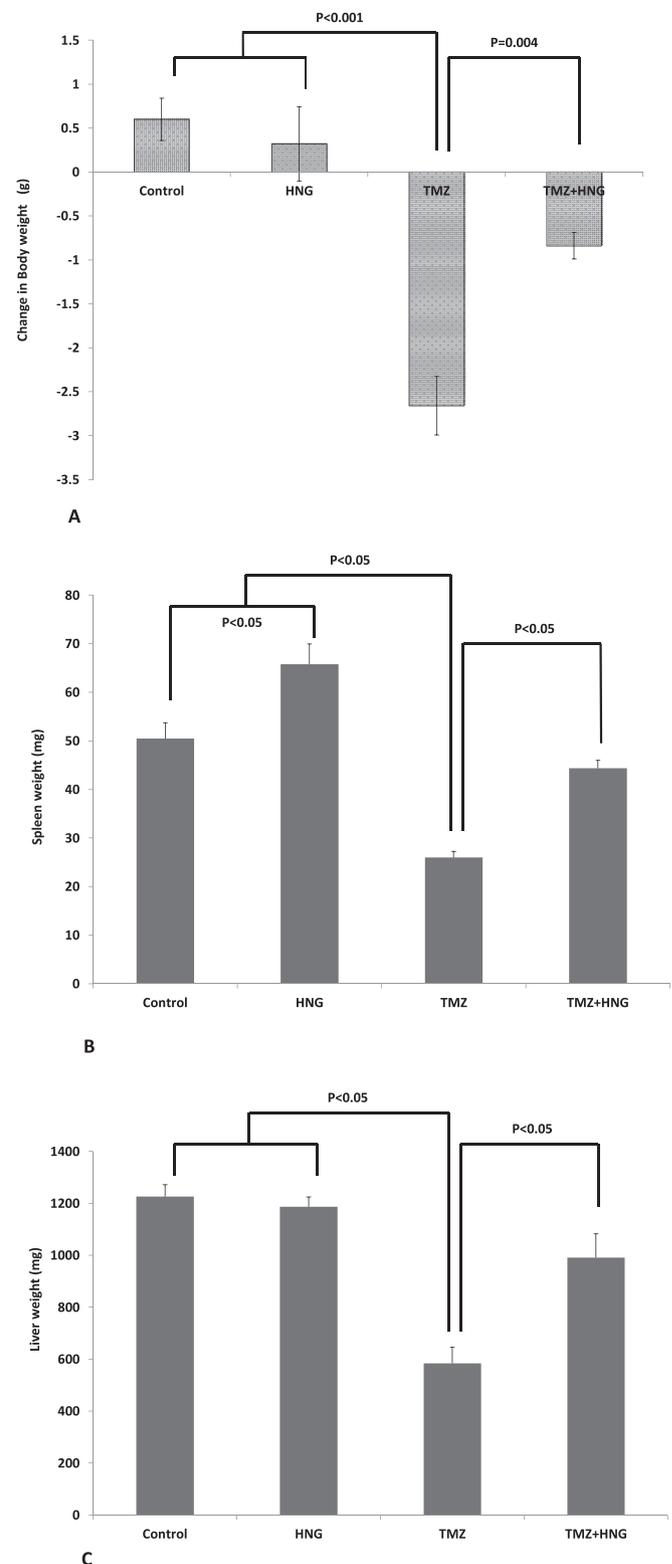

A

B

C

Fig. 1. Effect of HNG on Temozolomide (TMZ)-induced weight changes of body, spleen, and liver.

Mice were treated with vehicle (Control), HNG, TMZ, TMZ + HNG as described in experimental procedures ($n = 4$ in control, 5 each group in the rest). (A) HNG had no significant effect while TMZ significantly decreased body weights when compared to control. HNG significantly prevented TMZ-induced body weights loss ($P < .05$). (B) HNG alone increased spleen weights compared with control SCID mice. TMZ significantly decreased spleen weight which were prevented by combined HNG administration ($P < .05$). (C) HNG alone did not change liver weight while TMZ significantly decreased liver weight. HNG partially prevented TMZ-suppressed liver weights ($P < .05$). Values are
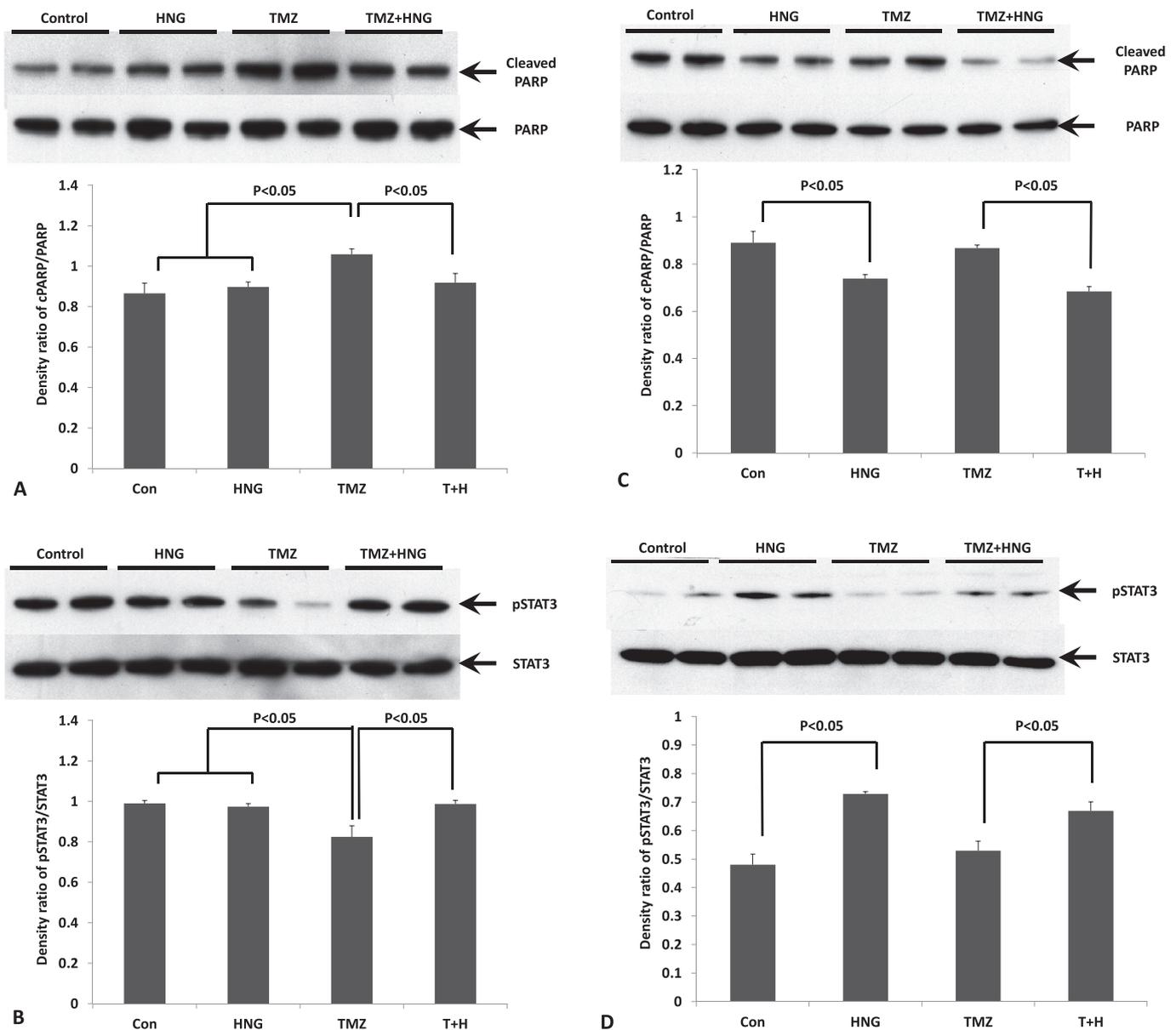
Fig. 2. Effects of HNG on Temozolomide (TMZ)-induced changes of cleaved PARP and phosphorylated STAT3 in liver and spleen.
Protein expressions in liver and spleen were measured by Western blots and optical density ratio was used to compare protein expression changes between different groups. (A) Changes of cleaved PARP in liver tissue. Compared with control, HNG alone did not change cleaved PARP. HNG significantly attenuated TMZ-increased cleaved PARP. Uncleaved PARP was used as nomalizer. (B) Changes of phosphorylated STAT3 in liver tissue. Compared with control, HNG alone did not change phosphorylation of STAT3. HNG significantly attenuated TMZ-suppressed STAT3 phosphorylation. STAT3 was not different in any treatment group. (C) Changes of cleaved PARP in spleen tissue. Compared with control, HNG suppressed cleaved PARP in SCID mice with or without TMZ treatment. Uncleaved PARP was used as nomalizer. (D) Changes of phosphorylated STAT3 in spleen tissue. Compared with control, HNG increased phosphorylation of STAT3 in SCID mice with or without TMZ treatment. STAT3 was not different in any treatment group. Values are means ± SEM.

phosphorylation of STAT3 (Fig. 2D, $p < .05$ compared with TMZ alone group).

3.3. HNG decreased TMZ-induced germ cell apoptosis in mouse testis via activation of STAT-3 and inhibition of p38 MAPK

Synthetic HNG peptide alone did not change the spontaneous germ cell apoptosis in SCID mouse. TMZ treatment increased germ cell apoptosis at both early + late (Fig. 3A, 0.12 ± 0.01 in TMZ group compared with control group 0.05 ± 0.01, $p < .01$) and middle (Fig. 3B, 0.06 ± 0.01 in TMZ group compared with control group 0.02 ± 0.01, $p < .01$) stages of seminiferous epithelial cycles in SCID mice. TMZ-induced germ cell apoptosis was significantly prevented by

HNG administration in both early + late stages (Fig. 3A, 0.06 ± 0.01 in TMZ + HNG group compared with TMZ group, $p < .05$) and in middle stages (Fig. 3B, 0.02 ± 0.01 in TMZ + HNG compared with TMZ group, $p < .05$).

Immuno-blot analyses on testis homogenates showed that HNG did not affect STAT3 phosphorylation and p38MAPK activation (Fig. 4A and B). TMZ treatment suppressed Ser727-phosphorylated STAT3 in testes (Fig. 4A, $p < .05$ compared with control group) but stimulated p38 MAPK phosphorylation reflected by increasing of ATF2 phosphorylation (Fig. 4B, $p < .05$ compared with control group). HNG administration restored TMZ-suppressed Ser 727-phosphorylation of STAT3 (Fig. 4A, $p < .05$ compared with TMZ alone group) and reduced TMZ-related p38 MAPK phosphorylation (Fig. 4B, $p < .05$
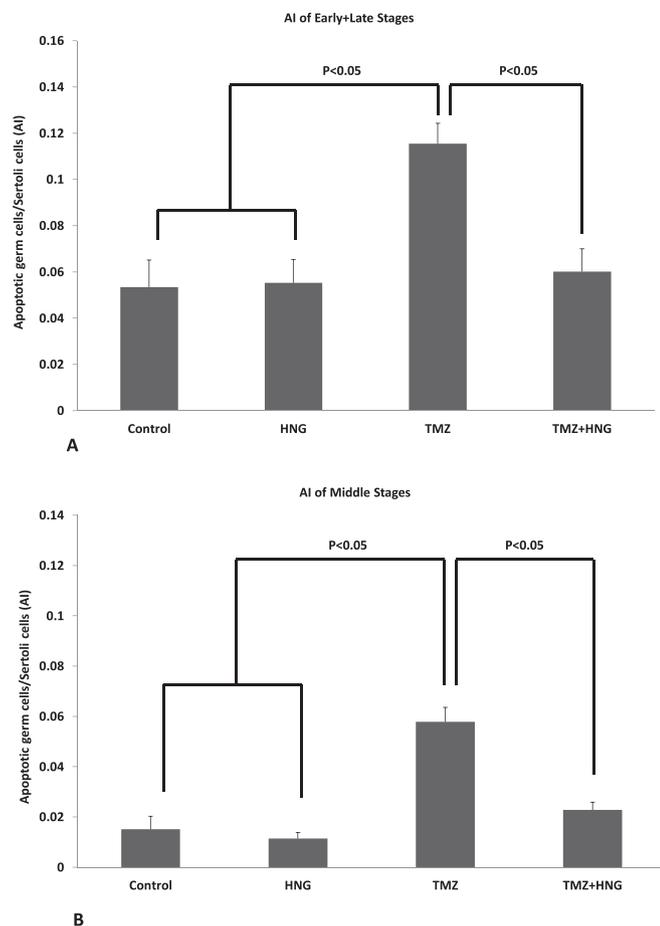
Fig. 3. Effect of HNG on Temozolomide (TMZ)-induced male germ cell apoptosis in SCID mice.

Quantification of apoptotic germ cells in early + late stages (A) and middle stages (B) in SCID mice testis. The rate of germ cell apoptosis is similar between control and HNG groups (p > .05). TMZ significantly increased the number of apoptotic cells compared with control (p < .05). HNG co-treatment significantly attenuated germ cell apoptosis induced by TMZ treatment (p < .05). Values are the mean ± SEM.

compared with TMZ alone group).

Our previous studies on testis showed that male germ cell apoptosis in response to stress occurs through mitochondria dependent pathway (Sinha Hikim et al., 1995; Jia et al., 2007; Jia et al., 2009). In present study, by using testis cytosol and mitochondria fractionations, we found that TMZ increased and HNG co-treatment reduced BAX in the mitochondrial fractions (Fig. 4C) and cytochrome C in the cytoplasm (Fig. 4D).

3.4. HNG reversed TMZ-induced decrease in white blood cells and granulocytes

Compared with wild type animal, the total number of white blood cells in SCID mouse is much lower mainly because markedly decrease in T and B lymphocytes (Gordon et al., 1991; Leblond et al., 1997; Matsumoto et al., 1995). HNG significantly increased the number of total WBC (Fig. 5A), granulocytes (Fig. 5B), but not lymphocytes (Fig. 5C), and monocytes (Fig. 5D). TMZ treatment did not significantly suppress the number of total WBC, lymphocytes, granulocytes, or monocytes compared to the control group. Addition of HNG to TMZ treated animals, similar to the controls, significantly increased total WBC and granulocytes (Fig. 5A and B, both p < .05) compared to TMZ treatment alone. There were no significant changes in red blood cell or

platelet counts between different groups (data not shown).

3.5. HNG did not alter the tumor suppressive effects of TMZ

Before treatment, the average tumor volumes were not different between groups (Fig. 6A). After treatment, synthetic HNG peptide alone did not change tumor size (Fig. 6B) or weight (Fig. 6C) in SCID mouse. TMZ treatment suppressed tumor growth as reflected by size (TMZ 7.72 ± 0.93 mm³, Control 14.28 ± 0.93 mm³, p < .01) (Fig. 6B) and by weight (TMZ: 4.80 ± 0.58 mg, control group, 23.75 ± 1.89 mg, p < .01) (Fig. 6C). HNG administration did not affect TMZ-induced tumor suppression assessed by tumor size (TMZ + HNG: 7.02 ± 0.73 mm³ (Fig. 6B), or weight, (TMZ + HNG: 4.60 ± 1.03 mg) (Fig. 6C).

4. Discussion

Infertility is amongst the most common long-term side effects of chemotherapy and preservation of fertility is important in cancer survivors (Tournaye et al., 2014; Trost and Brannigan, 2012). Chemotherapy results in decreased sperm output and reproductive capacity (Marcon et al., 2008; Meistrich, 2009; Delbes et al., 2010; Dohle, 2010). In boys, because cryopreservation of sperm is often not possible, testicular tissues may be experimentally cryopreserved and then later used for auto-transplantation for infertility with poor results (Lee and Shin, 2013; Armenian et al., 2013).

Humanin is a 24-amino acid mitochondria-derived peptide which has cytoprotective effects in many cells and tissues (Hashimoto et al., 2001; Bachar et al., 2010; Muzumdar et al., 2010; Eriksson et al., 2014; Wang et al., 2005; Lue et al., 2015; Jia et al., 2015). In previous studies, we showed that co-administration of HN or its potent analogue-HNG significantly reduced male germ cell apoptosis induced by two commonly used chemotherapeutic medications, cyclophosphamide and doxorubicin, in mouse models. Importantly the HN not only did not prevent tumor cells from chemotherapy-induced cell death but enhance the tumor suppressive effect of chemotherapy in a mouse metastatic melanoma tumor model (Lue et al., 2015).

This study differs from our prior studies in that a human tumor cell line from a common pediatric age malignancy was used with a different chemotherapeutic agent used currently in children. Because human cell line was implanted to mice, immunocompromised mice (SCID) were used as the host. Medulloblastoma is a common pediatric malignant primary brain tumor which requires maximal surgical removal of the tumor and is usually followed by radiation and chemotherapy to increase the disease-free survival. TMZ is a one of the choices in chemotherapy of childhood brain tumors. TMZ is an alkylating agent and thus may induce loss of germ cells and fertility. In present study, we used a model of subcutaneously implanted human medulloblastoma in SCID mice to explore the protective effect of HNG on male germ cells against TMZ and the effect of HNG on TMZ suppression of tumor growth. Our results proved that exogenous HNG had protective effects against TMZ-induced apoptosis in all stages of spermatogenesis in subcutaneous medulloblastoma tumor-bearing SCID mice. The action of HNG does not require presence of a functioning immune system.

We also studied the mechanism of HNG in preventing TMZ-induced male germ cell apoptosis. In neuronal cells, a putative membrane trimetric receptor (with three components: CNTFRα, WSX-1, and gp130) was reported that mediates the cytoprotective effects of HN via the STAT3 pathway (Hashimoto et al., 2005; Hashimoto et al., 2009; Matsuoka and Hashimoto, 2010). In this study, we found that TMZ induced male germ cell apoptosis in vivo by reducing pSTAT3 in the testis and HNG restored the TMZ-suppressed STAT3 phosphorylation. This is consistent with our previous finding that HN reduced stress-induced germ cell apoptosis by reversing the suppression of STAT3 phosphorylation (Jia et al., 2013; Jia et al., 2015) but enhances our understanding of the action even in the absence of a competent immune
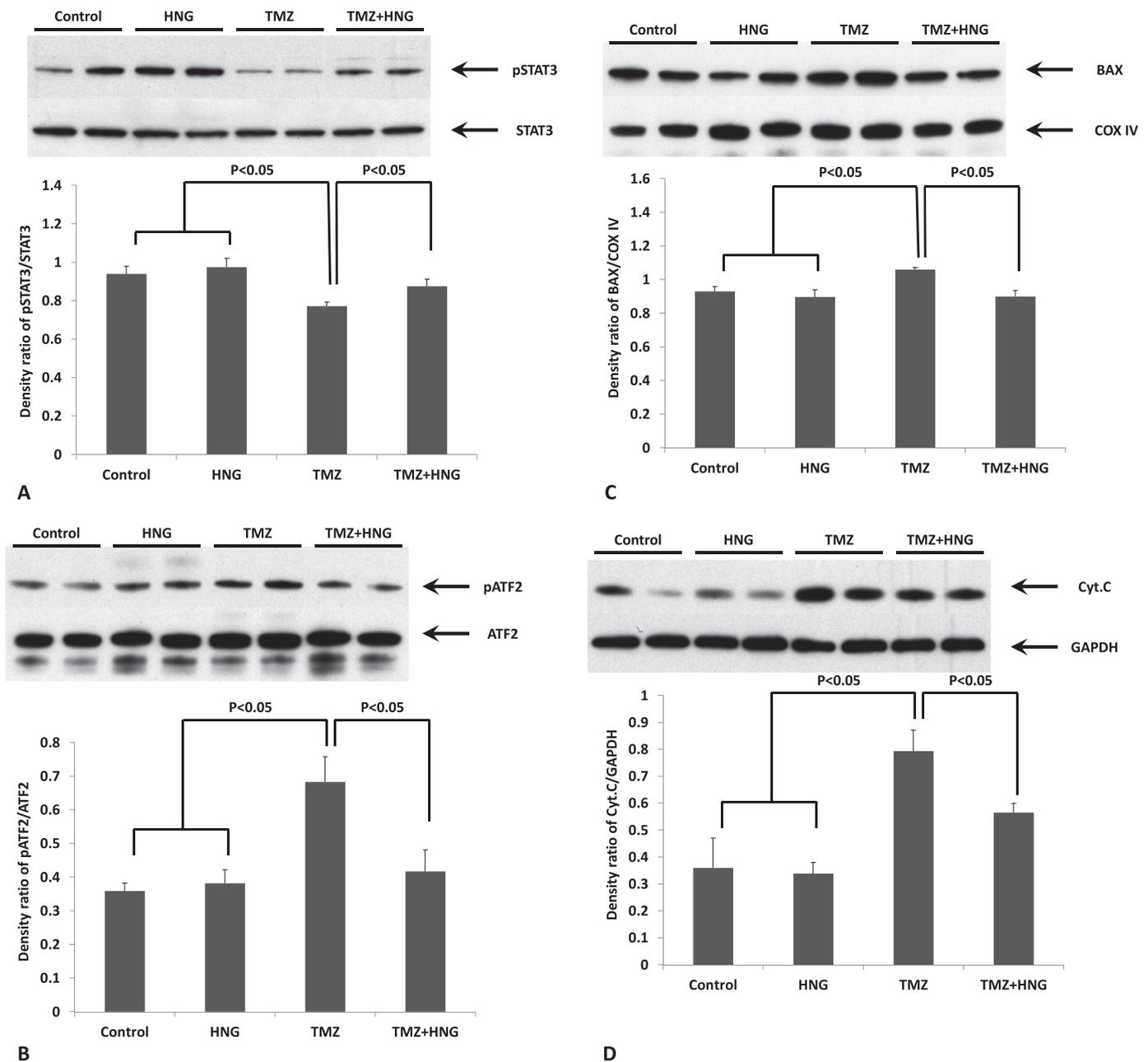
Fig. 4. Effect of HNG on Temozolomide (TMZ)-induced changes of STAT3, p38MAPK, BAX, and Cytochrome C in testis.
Protein expressions in testis were measured by Western blots and optical density ratio was used to compare protein expression changes between different groups. (A) Compared with control, HNG alone did not change phosphorylation of STAT3. HNG significantly attenuated TMZ-suppressed STAT3 phosphorylation. STAT3 was not different in any treatment group. (B) Change of p38MAPK phosphorylation were detected by an activity kit and presented by optical density ratio of phosphorylated ATF2/ATF2 as described in methods. Compared with control, HNG alone did not change phosphorylation of p38MAPK. HNG co-treatment significantly suppressed TMZ-induced p38MAPK activation. (C) Compared with control, HNG alone did not affect BAX expression in the mitochondria (COX IV as a loading control for mitochondrial fraction). HNG co-treatment prevented TMZ-induced BAX increase in the mitochondria. (D) Compared with control, HNG alone did not change cytochrome *c* expression in the cytoplasmic fraction. HNG co-treatment partially prevented TMZ-induced increased in cytochrome *c* in the cytoplasm. Values are means ± SEM.

system. Thus, we believe that STAT3 phosphorylation pathway is one of the important mechanisms for anti-apoptotic effect of HN in male germ cells.

We have previously reported p38 MAPK activation and downstream mitochondria-dependent apoptotic cascade is the main pathway for male germ cell apoptosis induced by stresses, such as heat and hormone deprivation (Jia et al., 2007; Jia et al., 2009; Vera et al., 2006). In this study, TMZ-activated p38MAPK phosphorylation was attenuated by co-administration of HNG. We further confirmed that HNG prevented TMZ-induced male germ cell apoptosis was mitochondria-dependent as

evidenced by HNG preventing the increase of BAX in the mitochondria and the increase of cytochrome C in the cytoplasm. Prior studies including our own showed that HN binds intracellularly to BAX sequestrating this pro-apoptotic protein in the cytoplasm preventing its entry to the mitochondria to initiate the apoptotic cascade (von Bueren et al., 2012; Zhai et al., 2005; Jia et al., 2010). This suggests that anti-apoptotic actions of HN in male germ cell are complex and may act through multiple pathways.

Our laboratory recently showed that HNG rescued cyclophosphamide-induced suppression of leucocytes in mice with metastatic
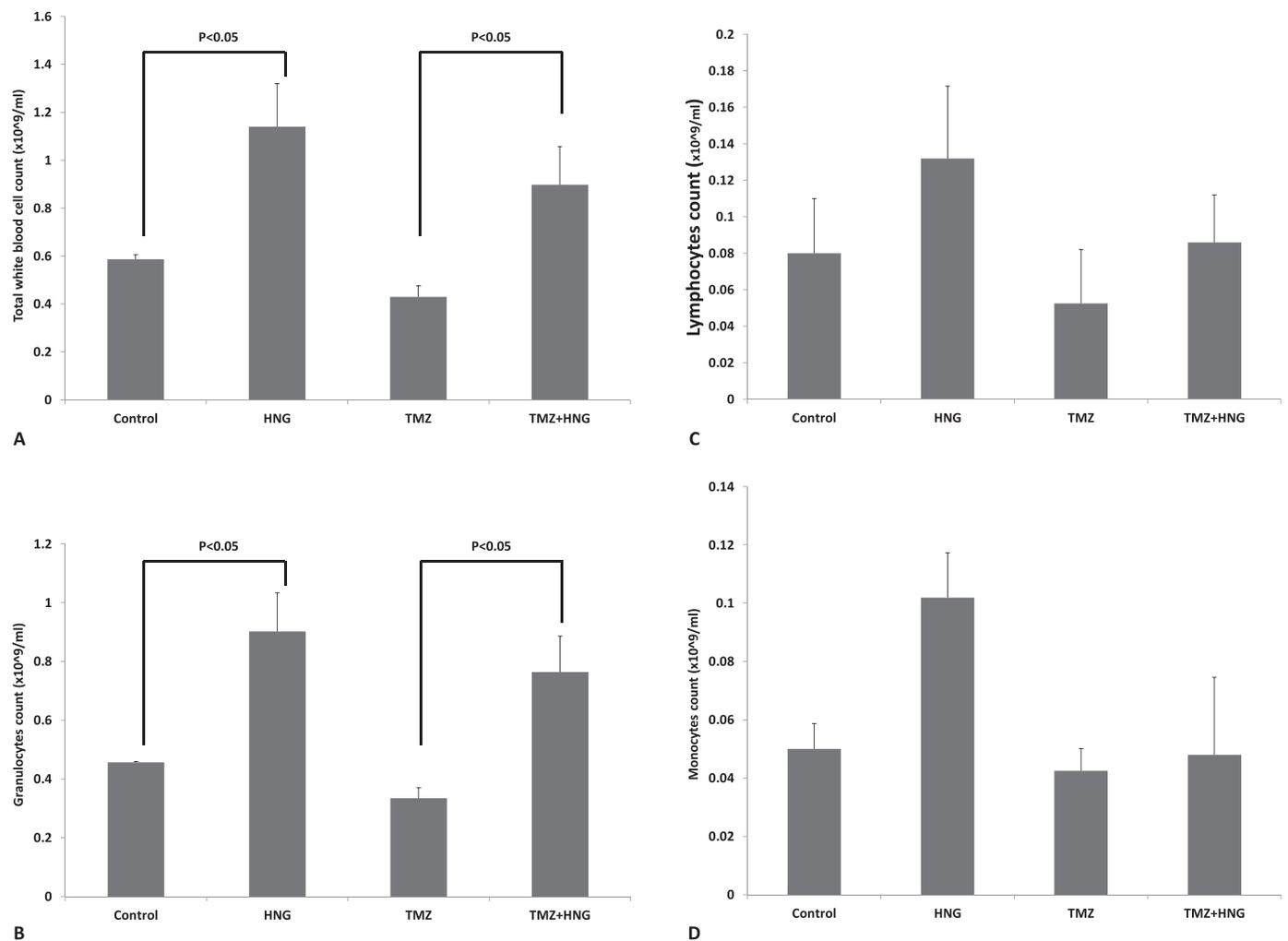
Fig. 5. Effect of HNG on white blood cell and differential counts in SCID mice.

Mice were treated with vehicle (Control), HNG, TMZ, TMZ + HNG as described in experimental procedures ($n = 3$ in control, 4 in TMZ group, and 5 each group in the rest). HNG alone increased total WBC (A) and granulocytes (B) compared with non-treated control SCID mice. Compared with control, TMZ did not suppress WBC but TMZ + HNG significantly increased WBC (A) and granulocytes number (B). No significant change was detected in lymphocytes (C) and monocytes (D) number between different groups. Values are means ± SEM.

melanoma (Lue et al., 2015). In the present model, SCID mouse has low numbers of circulating WBC due to a specific impairment of the differentiation of stem cells into mature lymphocytes without affecting myeloid cell differentiation (Bosma and Carroll, 1991; Dorshkind, 1991). The interesting and unexpected finding was that HNG treatment significantly increased the numbers of total WBC and granulocytes in SCID mice. HNG does not appear to have any significant effect on cells and tissues that are not under stress or damage. Thus it is possible that in the SCID mice bearing subcutaneous medulloblastoma, HNG increased WBC and granulocyte count because of the stress to the bone marrow by cancer or by the markedly the compromised immunity. TMZ may induce lymphopenia and myelosuppression leading to opportunistic infections in cancer patients (Sengupta et al., 2012; Niewald et al., n.d.; Fadul et al., 2011). But in our SCID mouse model, there was no suppression of total WBC or differential counts in TMZ treated animals compared with non-treated control group, which may be due to SCID mice have very low WBC and further suppression by TMZ was not evident.

In addition to the protective effect of HNG in TMZ-induced male germ cell apoptosis and white blood cell suppression in SCID mice, we found that the body, spleen and liver weights decreased significantly with TMZ treatment. HNG injections decreased the suppression of body and liver weights induced by TMZ. HNG protected TMZ-induced liver

damage likely through suppressing hepatocytes apoptosis pathway as shown by the decrease of TMZ-induced cleaved PARP, a marker of apoptosis. HNG also restored TMZ-suppressed STAT3 phosphorylation in liver tissue suggesting that HNG's protection against damage may be through binding to the putative IL-12 like receptor using STAT3 as its signaling mechanism.

SCID mouse has small spleen, small thymus glands, and tiny lymph nodes (Trost and Brannigan, 2012). Interestingly, HNG increased spleen weight of SCID mouse compared with non-treated control group and HNG also increased spleen weight in TMZ + HNG treated group compared with TMZ treated group. The results of cleaved PARP showed that there were massive apoptosis in SCID mice even without TMZ treatment such that further cell damage via apoptosis by TMZ treatment at the dose used in this study were not demonstrated in the spleen. HNG treatment protected spleen cells via suppressing apoptosis as reflected by decreasing the cleaved PARP in SCID mouse with or without TMZ treatment. We also showed that protective effect of HNG in spleen was related to the activation of STAT3 pathway which was consistent with the effect of HNG in testis and liver. Our observation of HNG increasing weight and decreasing apoptosis in the spleen of SCID mice may suggest the possible rescue effect of HNG in a severely compromised immune environment. Further studies are required to substantiate and clarify the action of HNG in an immunocompromised system in mouse. To our
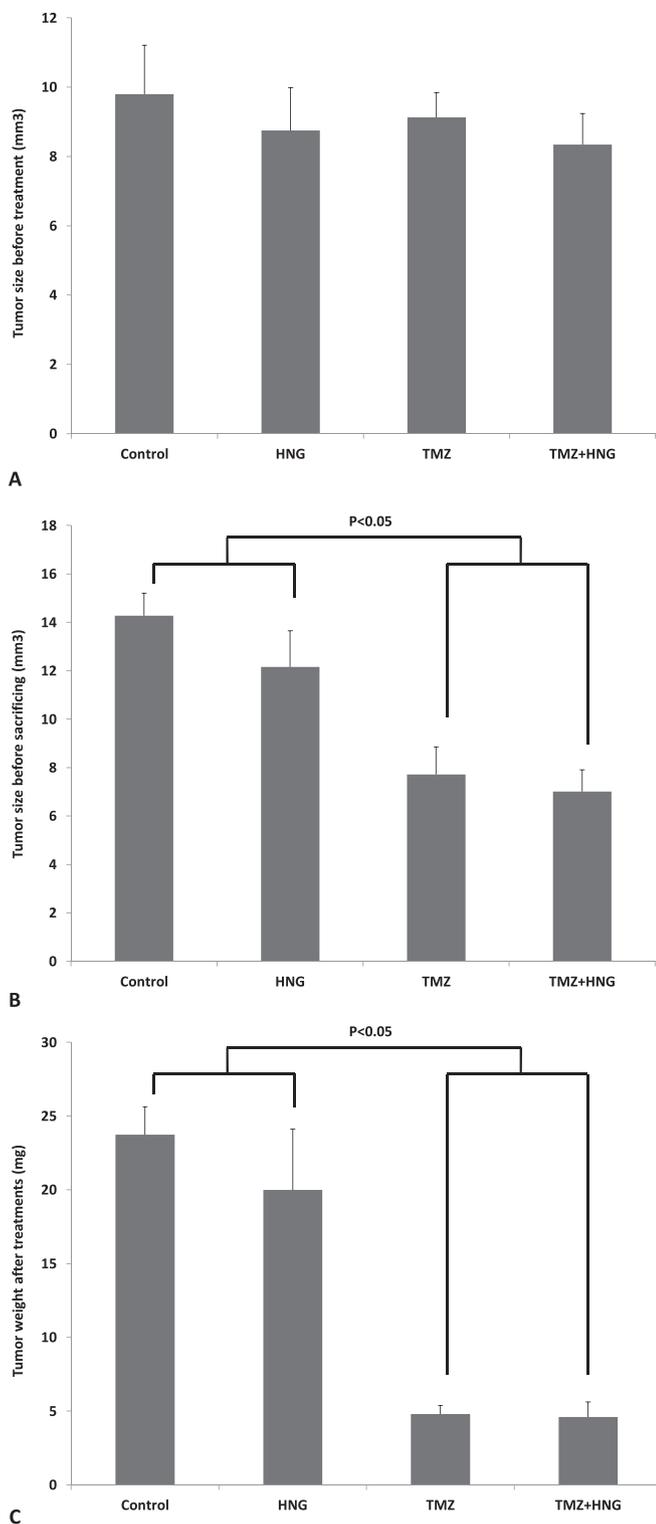
A

B

P<0.05

C

P<0.05

Fig. 6. HNG did not change anti-tumor effects of Temozolomide (TMZ). Mice were treated with vehicle (Control), HNG, TMZ, TMZ + HNG as described in experimental procedures (n = 4 in control, 5 each group in the rest). (A) Before treatment, there was no difference of tumor sizes between treatment groups. After treatment, tumor growth was measured by tumor size (B) and tumor weight (C). HNG alone did not change tumor size or weight compared with control SCID mice. TMZ significantly suppressed tumor growth. HNG-TMZ co-treatment did not further enhance TMZ-suppressed tumor growth. Values are means ± SEM.

knowledge, this is the first time that TMZ-induced body weight loss and decreased the weights of liver and spleen were reversed by HNG in SCID mice. Our current data in this SCID mice model suggest that protective effects of HNG against chemotherapyry-induced tissue and organ damage is not limited to the testis or WBC but also to vital organs such as the spleen and liver and expend the role of HN/HNG in cancer patients receiving chemotherapies (Cohen, 2014).

Another very important finding in this study was that HNG did not protect tumor cells from anti-tumor effects of TMZ. HNG-TMZ combined treatment did not enhance the tumor size or weight compared with TMZ treated group. In a prior report where neuroblastoma cells were implanted subcutaneously in nude mice (T lymphocytes deficiency with normal B lymphocytes), HNG did not interfere with the anti-tumor effects of a proteasome inhibitor, bortezomib, but HNG alone showed similar anti-tumor effects in their mice model (Eriksson et al., 2014). Our results in SCID mouse was also different from prior data from our laboratory showing HNG alone suppressed the number of metastatic tumors, and additively/synergistically enhanced the chemotherapy-induced melanoma tumor suppression in immunocompetent mice (Lue et al., 2015). The lack of synergistic action of HNG or anti-tumor effect in SCID mice in this study may due to 1) the difference in biologic response of melanoma versus medulloblastoma; 2) subcutaneous versus intravenous implanted tumors; 3) the antitumor activity of cyclophsopamide versus TMZ; and 4) the more severe suppression of the immune system in SCID (both T and B lymphocytes deficiency) compared to the nude or intact mice. Clearly more investigation is needed to study the role of humanin and HNG in different systems/organs including immune system; as adjuvant to different cancer chemotherapy methods, and also in different animal implanted-tumor models.

5. Conclusions

In summary, we demonstrated in the current study that 1) HNG significantly prevents TMZ-induced male germ cell apoptosis in SCID mice bearing subcutaneously implanted human medulloblastoma; 2) HNG increased the total WBC and granulocytes in SCID mice with or without TMZ treatment; 3) HNG prevents TMZ-induced body weight loss and prevents TMZ-suppressed liver and spleen weights through suppressing cell apoptosis in SCID mice; 4) HNG does not interfere with the beneficial anti-tumor effects of TMZ on subcutaneously implanted medulloblastoma in SCID mice. By studying the role of humanin and its analogs such as HNG in animals bearing different tumors may help to find specific targets which can be used for developing agonists to preserve fertility while protecting male germ cells from chemotherapy-induced cell loss and possibly toxic effects in other organs in cancer patients receiving chemotherapy.

Conflicts of interests

The authors have no potential conflicts of interest to disclose.

References

Armenian, S.H., Landier, W., Hudson, M.M., et al., 2013. Children's oncology Group's 2013 blueprint for research: survivorship and outcomes. Pediatr. Blood Cancer 60, 1063–1068.
Leblond, V., Autran, B., Cesbron, J.Y., 1997. The SCID mouse mutant: definition and potential use as a model for immune and hematological disorders. Hematol Cell Ther. 39, 213–221.
Bachar, A.R., Scheffer, L., Schroeder, A.S., et al., 2010. Humanin is expressed in human vascular walls and has a cytoprotective effect against oxidized LDL-induced oxidative stress. Cardiovasc. Res. 88, 360–366.
Bosma, M.J., Carroll, A.M., 1991. The SCID mouse mutant: definition, characterization, and potential uses. Annu. Rev. Immunol. 9, 323–350.
von Bueren, A.O.B.M., Hagel, C., Heinimann, K., et al., 2012. Mismatch repair deficiency: a Temozolomide resistance factor in medulloblastoma cell lines that is uncommon in primary medulloblastoma tumors. Br. J. Cancer 107, 1399–1408.
Cai, L., Hales, B.F., Robaire, B., 1997. Induction of apoptosis in the germ cells of adult

male rats after exposure to cyclophosphamide. Biol. Reprod. 56, 1490–1497.

Cohen, P., 2014. New role for the mitochondrial peptide Humanin: protective agent against chemotherapy-induced side effects. J. Natl. Cancer Inst. 106, dju006.

Delbes, G., Vaisheva, F., Luu, T., et al., 2010. Reversibility of the effects of the chemotherapeutic regimen for non-Hodgkin lymphoma, cyclophosphamide, doxorubicin, vincristine, and prednisone, on the male rat reproductive system and progeny outcome. Reprod. Toxicol. 29, 332–338.

Dohle, G.R., 2010. Male infertility in cancer patients: review of the literature. Int. J. Urol. 17, 327–331.

Dorshkind, K., 1991. In vivo administration of recombinant granulocyte-macrophage colony-stimulating factor results in a reversible inhibition of primary B lymphopoiesis. J. Immunol. 146, 4204–4208.

Eriksson, E., Wickström, M., Perup, L.S., et al., 2014. Protective role of humanin on bortezomib-induced bone growth impairment in anticancer treatment. J. Natl. Cancer Inst. 106, djt459.

Fadul, C.E., Fisher, J.L., Gui, J., et al., 2011. Immune modulation effects of concomitant temozolomide and radiation therapy on peripheral blood mononuclear cells in patients with glioblastoma multiforme. Neuro-Oncology 13, 393–400.

Gordon, B.E., Durfee, W.J., Bennett, M., et al., 1991. Differential white blood cell counts as a preliminary screen for severe combined immunodeficient congenic mice. Lab. Anim. Sci. 41, 255–257.

Hashimoto, Y., Niikura, T., Tajima, H., et al., 2001. A rescue factor abolishing neuronal cell death by a wide spectrum of familial Alzheimer's disease genes and Aβ. Proc. Natl. Acad. Sci. U. S. A. 98, 6336–6341.

Hashimoto, Y., Suzuki, H., Aiso, S., et al., 2005. Involvement of tyrosine kinases and STAT3 in Humanin-mediated neuroprotection. Life Sci. 77, 3092–3104.

Hashimoto, Y., Kurita, M., Aiso, S., et al., 2009. Humanin inhibits neuronal cell death by interacting with a cytokine receptor complex or complexes involving CNTF receptor α/WSX-1/gp130. Mol. Biol. Cell 20, 2864–2873.

Hoang, P.T., Park, P., Cobb, L.J., et al., 2010. The neurosurvival factor humanin inhibits beta-cell apoptosis via signal transducer and activator of transcription 3 activation and delays and ameliorates diabetes in nonobese diabetic mice. Metabolism. 59, 343–349.

Jacobsen, P.F., Jenkyn, D.J., Papadimitriou, J.M., 1985. Establishment of a human medulloblastoma cell line and its heterotransplantation into nude mice. J. Neuropathol. Exp. Neurol. 44, 472–485.

Jia, Y., Sinha Hikim, A.P., Swerdloff, R.S., et al., 2007. Signaling pathways for germ cell death in adult Cynomolgus monkeys (Macaca fascicularis) induced by mild testicular hyperthermia and exogenous testosterone treatment. Biol. Reprod. 77, 83–92.

Jia, Y., Castellanos, J., Wang, C., et al., 2009. Mitogen-activated protein kinase signaling in male germ cell apoptosis in the rat. Biol. Reprod. 80, 771–780.

Jia, Y., Lee, K.W., Swerdloff, R., et al., 2010. Interaction of insulin-like growth factor-binding protein-3 and BAX in mitochondria promotes male germ cell apoptosis. J. Biol. Chem. 285, 1726–1732.

Jia, Y., Lue, Y.H., Swerdloff, R., et al., 2013. The cytoprotective peptide humanin is induced and neutralizes Bax after pro-apoptotic stress in the rat testis. Andrology. 1, 651–659.

Jia, Y., Ohanyan, A., Lue, Y.H., et al., 2015. The effects of humanin and its analogues on male germ cell apoptosis induced by chemotherapeutic drugs. Apoptosis. 20, 551–561.

Friedman, H.S., Kerby, T., Calvert, H., 2000. Temozolomide and treatment of malignant glioma. Clin. Cancer Res. 6 (7), 2585–2597.

Lee, S.H., Shin, C.H., 2013. Reduced male fertility in childhood cancer survivors. Ann Pediatr Endocrinol Metab. 18, 168–712.

Lue, Y.H., Sinha Hikim, A.P., Swerdloff, R.S., et al., 1999. Single exposure to heat induces stage-specific germ cell apoptosis in rats: role of intratesticular testosterone (T) on stage specificity. Endocrinology. 140, 1709–1717.

Lue, Y., Wang, C., Liu, Y.X., et al., 2006. Transient testicular warming enhances the suppressive effect of testosterone on spermatogenesis in adult cynomolgus monkeys (Macaca fascicularis). J. Clin. Endocrinol. Metab. 91, 539–545.

Lue, Y., Swerdloff, R., Liu, Q., et al., 2010. Opposing roles of insulin-like growth factor binding protein 3 and humanin in the regulation of testicular germ cell apoptosis. Endocrinology. 151, 350–357.

Lue, Y., Swerdloff, R., Wan, J., et al., 2015. The potent Humanin analogue (HNG) protects germ cells and leucocytes while enhancing chemotherapy-induced suppression of Cancer metastases in male mice. Endocrinology. 156, 4511–4521.

Marcon, L., Hales, B.F., Robaire, B., 2008. Reversibility of the effects of subchronic exposure to the cancer chemotherapeutics bleomycin, etoposide, and cisplatin on spermatogenesis, fertility, and progeny outcome in the male rat. J. Androl. 29 (4).

Matsumoto, K., Inukai, S., Isaka, T., et al., 1995. Cell counts in peripheral blood and bone marrow of male C.B-17 scid/scid mice. Lab. Anim. 29, 218–222.

Matsuoka, M., 2009. Humanin: a defender against Alzheimer's disease? Recent Pat CNS Drug Discov. 4, 37–42.

Matsuoka, M., Hashimoto, Y., 2010. Humanin and the receptors for humanin. Mol. Neurobiol. 41, 22–28.

Meistrich, M.L., 2009. Male gonadal toxicity. Pediatr. Blood Cancer 53, 261–266.

Muzumdar, R.H., Huffman, D.M., Atzmon, G., et al., 2009. Humanin: a novel central regulator of peripheral insulin action. PLoS One 4, e6334.

Muzumdar, R.H., Huffman, D.M., Calvert, J.W., et al., 2010. Acute humanin therapy attenuates myocardial ischemia and reperfusion injury in mice. Arterioscler. Thromb. Vasc. Biol. 30, 1940–1948.

Niewald, M., Berdel, C., Fleckenstein, J., et al., 2011. Toxicity after radiochemotherapy for glioblastoma using temozolomide–a retrospective evaluation. Radiat. Oncol. 6, 141.

Reynolds, C.P.S.B., DeClerck, Y.A., Moats, R.A., 2005. Assessing growth and response to therapy in murine tumor models. Methods Mol. Med. 111, 335–350.

Russell, L., 1977. Movement of spermatocytes from the basal to the adluminal compartment of the rat testes. Am. J. Anat. 148, 313–328.

Sengupta, S., Marrinan, J., Frishman, C., et al., 2012. Impact of temozolomide on immune response during malignant glioma chemotherapy. Clin. Dev. Immunol. 2012, 831090.

Sinha Hikim, A.P., Wang, C., Leung, A., et al., 1995. Involvement of apoptosis in the induction of germ cell degeneration in adult rats after gonadotropin-releasing hormone antagonist treatment. Endocrinology 136, 2770–2775.

Sinha Hikim, A.P., Rajavashisth, T.B., Sinha Hikim, I., et al., 1997. Significance of apoptosis in the temporal and stage-specific loss of germ cells in the adult rat after gonadotropin deprivation. Biol. Reprod. 57, 1193–1201.

Tournaye, H., Dohle, G.R., Barratt, C.L., 2014. Fertility preservation in men with cancer. Lancet. 384, 1295–1301.

Trost, L.W., Brannigan, R.E., 2012. Oncofertility and the male cancer patient. Curr. Treat. Options in Oncol. 13, 146–160.

Vera, Y., Erkkilä, K., Wang, C., et al., 2006. Involvement of p38 mitogen-activated protein kinase and inducible nitric oxide synthase in apoptotic signaling of murine and human male germ cells after hormone deprivation. Mol. Endocrinol. 20, 1597–1609.

Villano, J.L., Seery, T.E., Bressler, L.R., 2009. Temozolomide in malignant gliomas: current use and future targets. Cancer Chemother. Pharmacol. 64 (4), 647–655.

Wang, D., Li, H., Yuan, H., et al., 2005. Humanin delays apoptosis in K562 cells by downregulation of P38 MAP kinase. Apoptosis. 10, 963–971.

Wang, C., Cui, Y.G., Wang, X.H., et al., 2007. Transient scrotal hyperthermia and Levonorgestrel enhance testosterone-induced spermatogenesis suppression in men through increased germ cell apoptosis. J. Clin. Endocrinol. Metab. 92, 3292–3304.

Xu, X., Chua, C.C., Gao, J., et al., 2006. Humanin is a novel neuroprotective agent against stroke. Stroke. 37, 2613–2619.

Ying, Y., Iribarren, P., Zhou, Y., et al., 2004. Humanin, a newly identified neuroprotective factor, uses the G protein-coupled formylpeptide receptor-like-1 as a functional receptor. J. Immunol. 172, 7078–7085.

Zhai, D., Luciano, F., Zhu, X., et al., 2005. Humanin binds and nullifies bid activity by blocking its activation of Bax and Bak. J. Biol. Chem. 280, 15815–15824.